Experimental Investigation of Electrostatic Effect on Bubble Behaviors in Gas-Solid Fluidized Bed

Kezeng Dong, Qing Zhang, Zhengliang Huang, Zuwei Liao, Jingdai Wang, and Yongrong Yang
Dept. of Chemical and Biological Engineering, State Key Laboratory of Chemical Engineering, Zhejiang University, Hangzhou 310027, China

DOI 10.1002/aic.14725
Published online January 12, 2015 in Wiley Online Library (wileyonlinelibrary.com)

Electrostatics and hydrodynamics in the fluidized bed are mutually affected, and excess accumulation of electrostatic charges has a severe impact on hydrodynamics. However, there is a serious lack of experimental investigation of electrostatic effect on hydrodynamics. This work provides a first insight into the electrostatic effects on bubble behaviors experimentally by injecting a trace of liquid antistatic agents (LAA) into a fluidized bed. Different amounts of LAA (0–50 ppm) were injected to make the electrostatic charges vary in a wide range and the bubble behaviors were investigated simultaneously. Results showed that the charges on particles decreased with increasing amount of LAA, which resulted in larger bubble sizes, stronger fluctuations of dynamic bed height, and less wall sheeting, respectively. The maximum reduction ratio of bubble sizes due to electrostatic effect was 21%. When particles were charged, the bubble sizes were significantly smaller than those estimated from the classical correlation. This discrepancy was attributed to the neglect of electrostatic effect in classical correlation. © 2015 American Institute of Chemical Engineers *AIChE J*, 61: 1160–1171, 2015

Keywords: fluidized bed, electrostatics, liquid antistatic agent, gas bubble behaviors

Introduction

Electrostatic charges are generated and accumulated mostly due to insulated particle–particle and particle-wall frictions in the gas-solid fluidized bed. The excess accumulation of electrostatic charges has a severe impact on hydrodynamics in fluidized bed, even causes particle agglomeration and wall sheeting.[1,2] Recent research of electrostatics in fluidized bed mainly focuses on charge generation mechanism based on different electrostatic measurements. Boland and Geldart[3] studied the effects of mean particle size and gas humidity on charge generation and dissipation in the fluidized bed through ball electrostatic probes. They concluded that electrification in fluidized bed is generated by the motion of particles around bubbles. Park et al.[4] developed a single bubble injection experiment and found electrostatic charges in the fluidized bed increased as the bubble size increased. Zhao et al.[5] measured the charge distribution of fluidized particles using a vertical array of Faraday pail sensors and indicated that particles were bipolar charged and small particles tended to be negatively charged. Mehrani et al.[6] developed an on-line Faraday cup fluidized bed system and concluded that friction between gas and wall had little influence on electrostatic charges, while elutriation of fines was the main cause of charge accumulation in the fluidized bed. A technique has been developed by Chen et al.[7,8] to measure the charge distribution around a single rising bubble in a two-dimensional fluidized bed using a number of induction probes. Their results indicated that the wake of the bubble was more negatively charged than the emulsion phase, and a nearly zero charge density inside the bubble was found. Sowinski et al.[9,10] used a unique online Faraday cup method to measure the electrostatic charges of the bed particles, the particles adhered to the column wall, and the entrained fine particles. They found an occurrence of bipolar charging in both bubbling and slugging regimes with entrained fines being mainly positively charged, whereas the bed particles and those attached to the wall carried net negative charges.

According to the research mentioned previously, the change of hydrodynamics will certainly alter the degree of particle electrification.[11–15] However, the influence between hydrodynamics and electrostatics is mutual, and variation of charges on particles will also affect hydrodynamics in the fluidized bed. Unfortunately, there is a serious lack of experimental investigation of electrostatic effect on hydrodynamics. This is attributed to the fact that tribocharging of particles strongly depends on many factors, including physical properties of gas and solid, operating conditions, and environmental conditions.[1,16] A slight change of any of these factors will alter the electrostatics in the fluidized bed. Thus, tribocharging of insulated particles is not very easily to be controlled, which raises the difficulty in quantitatively adjusting the degree of electrification in the experimental investigation. Even so, some efforts have still been made to adjust the electrostatic charge in fluidized bed quantitatively. Reduction of electrostatic charge by increasing the humidity of fluidizing gas was investigated by Park et al.[4] and their

Correspondence concerning this article should be addressed to: J. Wang at wangjd@zju.edu.cn.

results indicated increasing the relative humidity reduced the electrostatic charge by increasing the surface conductivity of insulated particles. Relative humidity between 40 and 80% was the best for charges elimination, while over-humidification led to excessive capillary forces causing defluidization. Wang et al.[17] found the addition of a small amount of metal oxides into the fluidized bed can adjust the charge magnitude and polarity of particles. However, the physical property of fluidized particles was changed in the meantime and fines elutriation also increased. So far, due to the difficulty of experimental investigation, electrostatic effects on hydrodynamics in the fluidized bed have only been studied through numerical simulation. Rokkam et al.[18] developed a multifluid computational fluid dynamic (CFD) simulation coupled with an electrostatic model and found the entrainment rate reduced when fines were charged. Their simulation results of electrostatic effect on elutriation are in accordance with Briens[19] and Li[20]'s experimental results. Jalalinejad et al.[21] numerically investigated the effect of charged particles on single rising bubbles through two fluid model and found bubbles elongated and rose slowly when particles were charged. Hassani et al.[22] developed a discrete element method (DEM) coupled with CFD model to study the effect of electrostatic forces on fluidization hydrodynamics. Their results indicated that when particles were mono-charged, the repulsive forces between particles resulted in a larger emulsion voidage and smaller bubble sizes. Lim[23] developed a DEM study on the mixing behaviors in gas-solid fluidized bed systems with electrostatic effects and indicated that particles adhered to walls and less vigorous fluidization was found when the electrostatic forces between particle-wall were stronger than fluid drag forces.

Numerical simulation coupled with electrostatic model, to some extent, can obtain the electrostatic effect on fluidization hydrodynamics. However, most simulations have not been validated with experimental verification. Moreover, most simulations involve numerous assumptions and simplifications which seem unreasonable according to experimental results.[6,24–27] For instance, charge generation and dissipation are often neglected in electrostatic model and the amounts of charge on particles are assumed to be constant and independent of particle sizes. All these disadvantages limited the accuracy and applicability of simulation results. Therefore, it is of vital importance to investigate the electrostatic effects on hydrodynamics experimentally.

This work provides a first insight into the electrostatic effects on hydrodynamics experimentally, especially bubble behaviors, by injecting a trace of liquid antistatic agents (LAA) into the fluidized bed. Different amounts of LAA (0–50 ppm) were injected to make the electrostatic charges vary in a wide range (0–2.8 nC/g) and the bubble behaviors were investigated simultaneously. The influence of electrostatic charges on dynamic bed heights was also studied. The electrostatic effects on fluidization hydrodynamics were concluded and the affecting mechanism was also discussed.

Experimental Methods and Materials

Figure 1 shows the schematic diagram of experimental apparatus, which consists of fluidization system and detection system. The black solid line stands for gas flow and the dashed line represents the signal flow. The fluidized bed is made of a transparent Plexiglas column with an inner diameter of 150 mm and a height of 1000 mm, including an expanded section at the top, which has a height of 300 mm and a width of 250 mm. The bed column is equipped with a gas mixing chamber at the bottom and an iron perforated distributor with an open area ratio of 2.6%. The compressed air is dried and measured successively before entering the mixing chamber.

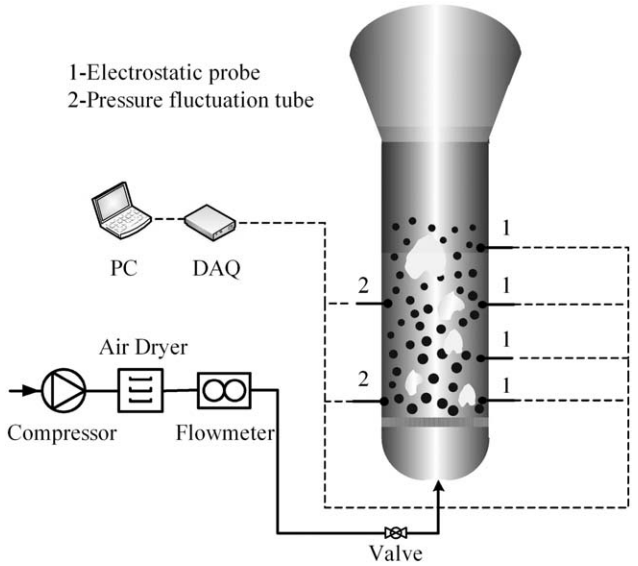

Figure 1. Schematic diagram of experimental apparatus.

The detection system includes electrostatic voltage measurement, Faraday cup electrometer and pressure fluctuation probe. The self-developed electrostatic voltage measurement consists of spherical electrostatic probe, voltage/current converter (ADTECH, MVX106), data acquisition card (NI, USB-6351), and computer. Output voltage signals were sampled at 400 Hz. The electrostatic probes were installed at various axial heights (80, 140, 190, and 240 mm) above the gas distributor and each probe was located 5 mm from the inner column wall. The Faraday cup electrometer (Monroe Electronics, NanoCoulomb Meter 284) was used to measure the average charge-to-mass ratio of charged particles. The sampling ports were set at 80 and 240 mm above the distributor. The charged particles from sampling port went directly into the Faraday cup due to the pressure difference between inside and outside of the fluidized bed. Considering the possible influence of sampling process on measurements, all experimental runs were repeated at least three times to ensure the reproducibility of the results. The pressure fluctuation signals were measured at 20, 160, and 240 mm above the distributor using three pressure tubes made of steel with a length of 80 mm and an internal diameter of 4 mm. Each pressure tube was mounted flush with the inner wall of the column with a fine mesh covering the tip to prevent fine particles from entering into the probe. The probe was connected to one of two channels of a differential pressure transducer (CTG121P, China), which produced an output voltage proportional to the pressure difference between the two channels. The other channel was exposed to the atmosphere. The measuring range of the pressure transducer is ± 2 kPa, and its relative accuracy is $\pm 0.25\%$ of full scale. The sampling frequency was 400 Hz in all cases and the signal was resampled to 100 Hz before further analysis. The locations of signal measuring points are specified in Figure 2.

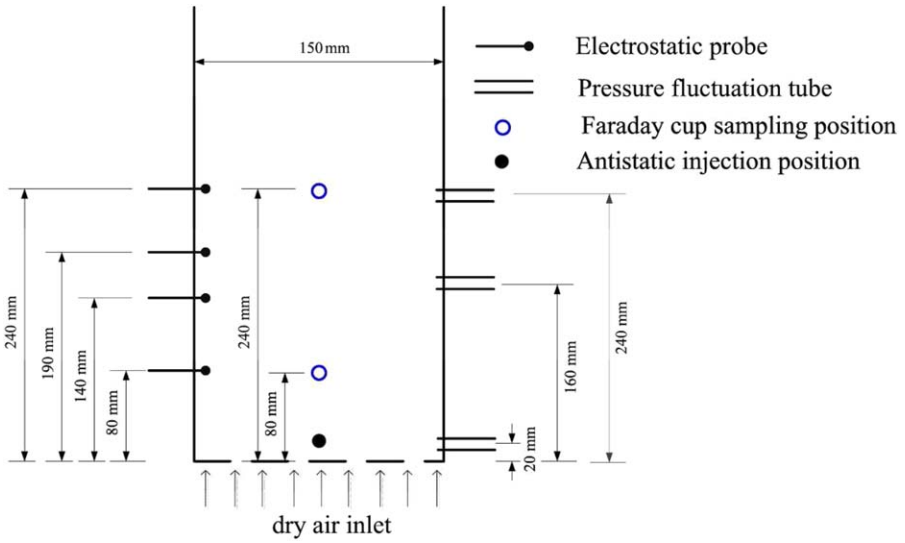

Figure 2. Locations of signal measuring points and antistatic injection.

[Color figure can be viewed in the online issue, which is available at wileyonlinelibrary.com.]

Atmer™ 163 is a synthetic ethoxylated amine in liquid form with a density of 0.86 g/cm^3, which is commonly used as antistatic agent in polyolefin. To avoid its larger concentration in a certain position, a trace of LAA was injected into the center of the bed close to the distributor so that LAA could be easily diffused with the help of high speed gas jet near the distributor, as shown in Figure 2. The amount of LAA added is listed in Table 1, and the mass ratio is calculated based on 2 kg particles. Since the amount of LAA added is less than 100 ppm, the influence of liquid itself on hydrodynamics can be neglected.[28]

Compressed air was used as fluidizing gas and predried to a relative humility of 10–15% and the air temperature was among 15–20°C. The polypropylene (PP) powder (Sinopec, China) with a particle density of 0.9 g/cm^3 was used as fluidized particles. PP powder has a mean diameter of 1.85 mm and belongs to Geldart D particles. The sieve size distribution of PP is displayed in Table 2.

Two fundamental experiments were carried out to study the triboelectric charging characteristic of PP particles over column wall.

First, a vibration test was developed to determinate the charge polarity of PP particles after impacting with polymethyl methacrylate (PMMA) wall. A certain weight of PP particles (the same PP particles used for fluidization) were put into a PMMA column with a diameter of 60 mm and a height of 200 mm. Then the PMMA column with PP particles was put on a vibrating device. After vibrating for 5 min, PP particles were moved into a Faraday cup, from which the charge to mass ratios were measured. The process was repeated for three times for each sample.

Second, to indicate the difference between the PP particles before and after injection of LAA, PP particles with different amounts of LAA were first melt and remodeled into a slice with a diameter of 80 mm and a thickness of 2 mm. The surface resistivity of PP slices was then measured by a high insulation tester (ZC90F, China). By applying a high voltage of 500 V on each slice for 1 min, the resistivity was acquired from the tester. Each sample was tested for at least three times to reduce the probability of detection errors.

The fluidized bed was first swept by dried air for 10 min, and 2 kg previously dried PP powder was added, with a static bed height of 210 mm. The particles were fluidized for at least 30 min to ensure fully tribocharging. The electrostatic voltage and pressure fluctuations were recorded simultaneously. When the electrostatic charges of particles reached equilibrium, particles were sampled and charge-to-mass ratios were measured. Then, a trace of LAA was injected near the distributor and variations of electrostatic voltage and pressure fluctuations were recorded again. Besides, a digital camera (Sony HDR-SR10) was used to record the bed surface during the experiment, at the speed of 25 frames/s and resolution of 1440 × 1080 pixels.

All the experiments in this work were carried out under a superficial gas velocity of 0.7 m/s. The minimum fluidization velocity (u_{mf}) was determined experimentally by the classical method (pressure drop across the bed vs. the decreasing superficial gas velocity). The value of u_{mf} was 0.54 and 0.47 m/s for fully charged particles and particles whose charges were eliminated by LAA, indicating an increase of u_{mf} for charged particles. The electrostatic forces between charged particles and particles adhered to walls obstructed normal fluidization, which resulted in an increase in u_{mf}. Besides, the transition velocity from bubbling to turbulent fluidization was independently studied by pressure fluctuations and found to be 1.77 m/s in this work.

Results and Discussions

Electrostatic charges control via LAA injection

When the superficial gas velocity was 0.7 m/s, the variations of electrostatic voltage at various axial bed heights

Table 1. Amount of LLA Added

Mass ratio, (ppm)	12.5	25	37.5	50	75	100
Volume, (mL)	0.03	0.06	0.09	0.12	0.18	0.24

Table 2. Size Distribution of PP Powder

Sieve size, (mm)	2.05	1.4	1	0.85	0.5	0.25	<0.25
Mass ratio, (%)	58.4	20.5	13.9	2.60	4.01	0.42	0.17

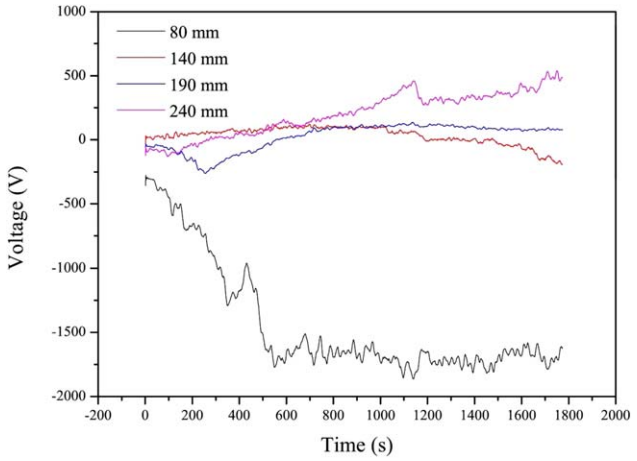

Figure 3. Variations of electrostatic voltage with fluidization time.

[Color figure can be viewed in the online issue, which is available at wileyonlinelibrary.com.]

with fluidization time were shown in Figure 3. The voltage at 80 mm above the distributor decreased rapidly with fluidization time and reached a minimum voltage 10 min later, indicating negatively charged particles at the bottom. The positive voltage at 240 mm increased slowly with fluidization time. According to Figure 1, the PP particles in the fluidized bed were bipolar charged, with negatively charged particles at the bottom part and positively charged particles at the top part. Besides, the negative voltage (absolute value) was significantly larger than positive voltage, indicating that most particles were negatively charged.

When the electrostatic voltage reached equilibrium, a trace of LAA was injected close to the distributor. Figure 4 showed the variations of electrostatic voltage after injection of 37.5 ppm LAA. After injection of LAA, the absolute value of voltage at 80 mm decreased rapidly at first and reached a relatively low voltage finally. For measuring points higher than 80 mm, the voltages increased rapidly and reached a peak, then decreased gradually to zero. Change of voltages at 80 and 240 mm were more significant compared with other measuring points. The

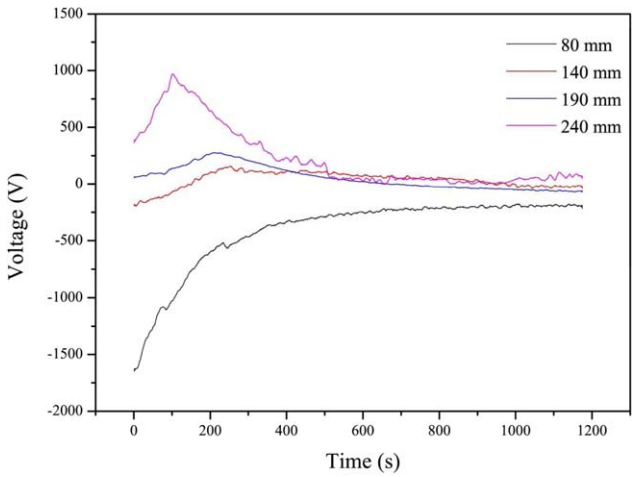

Figure 4. Variations of electrostatic voltage after LAA injection (37.5 ppm).

[Color figure can be viewed in the online issue, which is available at wileyonlinelibrary.com.]

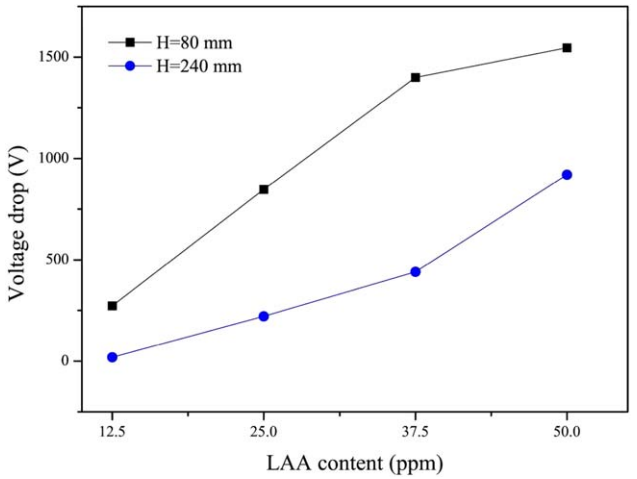

Figure 5. Electrostatic voltage drop under various LAA contents.

[Color figure can be viewed in the online issue, which is available at wileyonlinelibrary.com.]

following analyses were based on the variations of voltage at these two measuring points.

LAA has good conductivity since ethoxylated amine has hydrophilic group (—OH). Therefore, the surface charge dissipation rate of fluidized particles accelerated after injection of LAA, thus resulted in a decrease of electrostatic voltages in the fluidized bed. The charge dissipation rate of insulated particles strongly depends on the permittivity and resistivity, and the charge dissipation equation can be expressed as[29,30]

$$\frac{dQ}{dt} = -\frac{Q}{\tau_r} \tag{1}$$

τ_r is a time constant of charge dissipation and defined as,

$$\tau_r = \varepsilon_a \rho \tag{2}$$

where ε_a is the permittivity of insulated particles and ρ stands for resistivity. The differential Eq. 1 can be easily solved, as shown

$$Q = C \cdot e^{-t/\tau_r} \tag{3}$$

where C is a constant. According to Eqs. 1 and 2, a lower resistivity indicates a smaller time constant of charge dissipation, which means a faster charge dissipation rate.

Figure 5 displayed the variations of electrostatic voltage drop before and after injection of different amounts of LAA. The voltage drop was defined as the absolute difference between electrostatic voltage before and after injection of LAA. When injecting only 12.5 ppm LAA, there was almost no significant change of voltage at 240 mm, while the voltage at 80 mm reduced slightly. This is because the content of LAA was too low to diffuse effectively to the whole bed. Therefore, electrostatic voltage decrease was only observed at the bottom part of the fluidized bed, as the injection point was close to the distributor. With the increased amount of LAA injected, the electrostatic voltage drop increased significantly. When the content of LAA was larger than 37.5 ppm, the voltage drop increased to 1400 V at 80 mm height and the electrostatic voltage almost reached zero (as shown in Figure 4), which indicated that charges of particles were close to be completely eliminated.

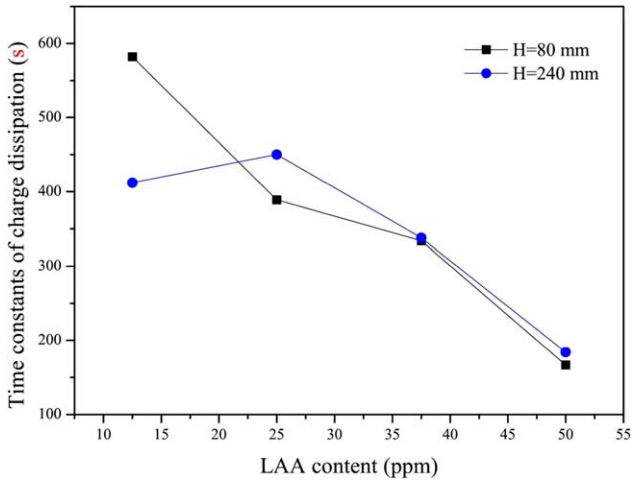

Figure 6. Time constants of charge dissipation under various contents of LAA.

[Color figure can be viewed in the online issue, which is available at wileyonlinelibrary.com.]

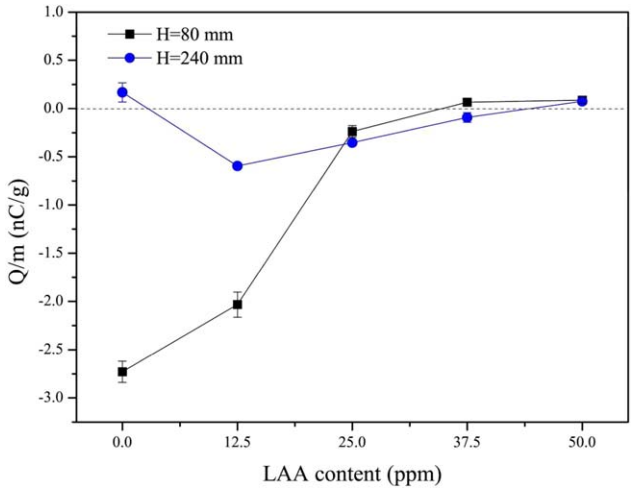

Figure 8. Variations of charge-to-mass ratios under various LAA contents.

[Color figure can be viewed in the online issue, which is available at wileyonlinelibrary.com.]

The time constants of charge dissipation after injection of LAA can be acquired through fitting of electrostatic voltage in Figure 4 by using Eq. 3. The fitting results are displayed in Figure 6. According to the figure, the time constants of charge dissipation decreased with the increasing LAA content, which indicated that a larger content of LAA injected resulted in a larger charge dissipation rate. According to Eqs. 1 and 2, the charge dissipation rate was inversely proportional to the surface resistivity of charged particles. When LAA was injected and fully diffused, the charged particles were covered with a conductive liquid film, which leaded to a decrease in surface resistivity. Therefore, a smaller time constant was found under a higher LAA content.

Besides, the time constant of charge dissipation at the top section did not change significantly when the injection content was less than 25 ppm. This was attributed to the fact that the injection position was close to the gas distributor and too little LAA was not able to reach the particles at the top section.

Figure 7 further shows the variation of surface resistivity of PP under various contents of LAA. The magnitude of the surface resistivity of PP was among 10^{13} Ω and decreased significantly after injection of LAA. When the injection content reached 100 ppm, the value of surface resistivity dropped 1.5 orders of magnitude. This was the main cause of electrostatic voltage decrease. The function of LAA as charge dissipation additives was similar to the effect of increasing gas humidity.[4,30,31]

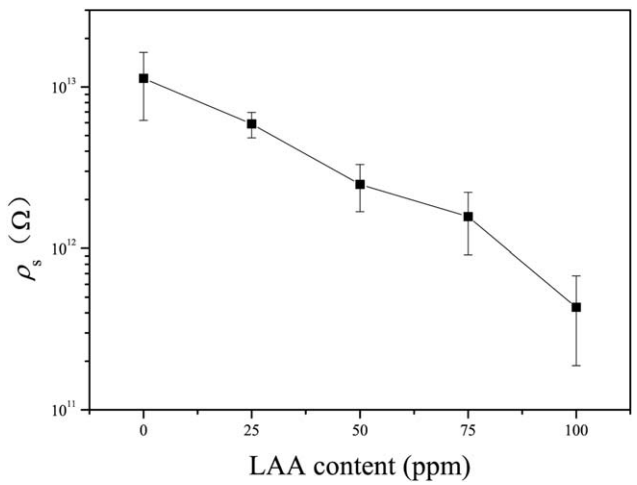

Figure 7. Surface resistivity of PP under various contents of LAA.

To further verify the influence of LAA on electrostatic charges in the fluidized bed, the variations of charge-to-mass ratios of particles were also measured. The results are displayed in Figure 8. When fully fluidized and charged, the particles at the bottom have an average charge-to-mass ratio of −2.75 nC/g, while the particles at the top have only 0.2 nC/g. The results indicated that particles were mainly negatively charged at the bottom and slightly positively charged at the top of the fluidized bed, which was consistent with the results of electrostatic voltages.

Moreover, the particles were more negatively charged. This was attributed to the contact potential difference between the particles and wall. Figure 9 indicated the mean charge to mass ratio of PP particles of different weight after impacting with PMMA column in the vibration test. When 2 g PP particles were continuously vibrated for 30 s and 5 min, Q/m reached −8.36 and −21.9 nC/g, respectively, which indicated an increase of charge on the particles due to continuous contact with PMMA wall. PP particles were negatively charged after impacting with PMMA wall, as predicted, since PP has a larger work function than PMMA.[32] Moreover, the mean absolute charge to mass ratio decreased with increasing PP weight. This is because that the particle–particle interactions resulted in bipolar charges, which reduced the overall mean absolute charge to mass ratio.

When LAA was injected into the fluidized bed, the surface charge dissipation rates of all particles increased. In addition, the smaller particles in the top section, which were mainly positively charged, had a larger dissipation rate than the large and negatively charged particles due to a larger specific surface area. Therefore, after injection of LAA, the fluidized bed displayed a mean negative charge at the upper part. Increasing the content of LAA leaded to a decrease in charge-to-mass ratios of both particles at the upper and lower

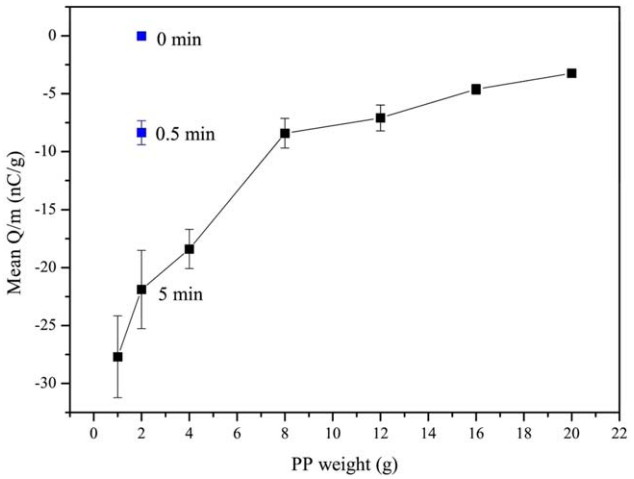

Figure 9. Mean charge to mass ratio of PP particles after impacting with PMMA column.

[Color figure can be viewed in the online issue, which is available at wileyonlinelibrary.com.]

part of bed. When the injection content reached 37.5 ppm, all the particles were close to be completely neutralized. Therefore, according to the results of electrostatic voltage and the charge-to-mass ratios, electrostatic charges in the fluidized bed can be controlled through injecting a trace of LAA.

The negatively charged particles were inclined to move toward the wall due to the electrostatic attractive forces and thus caused wall sheeting.[10,12,33,34] Figure 10 further shows the photos of wall sheeting in the fluidized bed after injection of LAA. As shown in Figure 10a, when particles were freely fluidized, severe wall sheeting was found on the whole internal wall. After injection of LAA, wall sheeting was obviously reduced due to a decrease of charges. Most sheeting disappeared when injecting 25 ppm LAA, except for a small zone about 50 mm above the distributor. This small area were called stagnant zone, in which particles were less active.[35,36] Therefore, in this section, a smaller electrostatic force can make particles adhere to the wall and particles already adhered were harder to drop from the wall. When injecting 50 ppm LAA, particles were completely neutralized and no sheeting was found on the wall. The variations of wall sheeting further verified the feasibility of charge control via injection of LAA.

In summary, PP particles were mainly negatively charged in the freely bubbling fluidized bed. Injecting a trace of LAA caused obvious decrease of electrostatic charges and disappearance of wall sheeting. According to the variations of electrostatic voltage, charge-to-mass ratios and wall sheeting, it is feasible to control the electrostatic charges in the fluidized bed through adding LAA.

Electrostatic effect on bubble behaviors

The first part of our work focuses on the feasibility of charge control, while this part of work focuses on the study of electrostatic effect on bubble behaviors. Pressure fluctuations were used to characterize the gas bubble behaviors under different charges.

Figure 11 first shows the pressure fluctuations in 10 s at 160 mm above the distributor under various contents of LAA. A large periodicity of pressure signal was found when particles were charged, and the peak values of the fluctuations were relatively uniform. As has been analyzed previously, particles were bipolar charged and tended to adhere to the wall when no LAA was injected into the fluidized bed. During experiments, an obvious decrease of dynamic bed height was observed after fluidization for 30 min. When adding 12.5 ppm LAA, no significant change of pressure fluctuations was

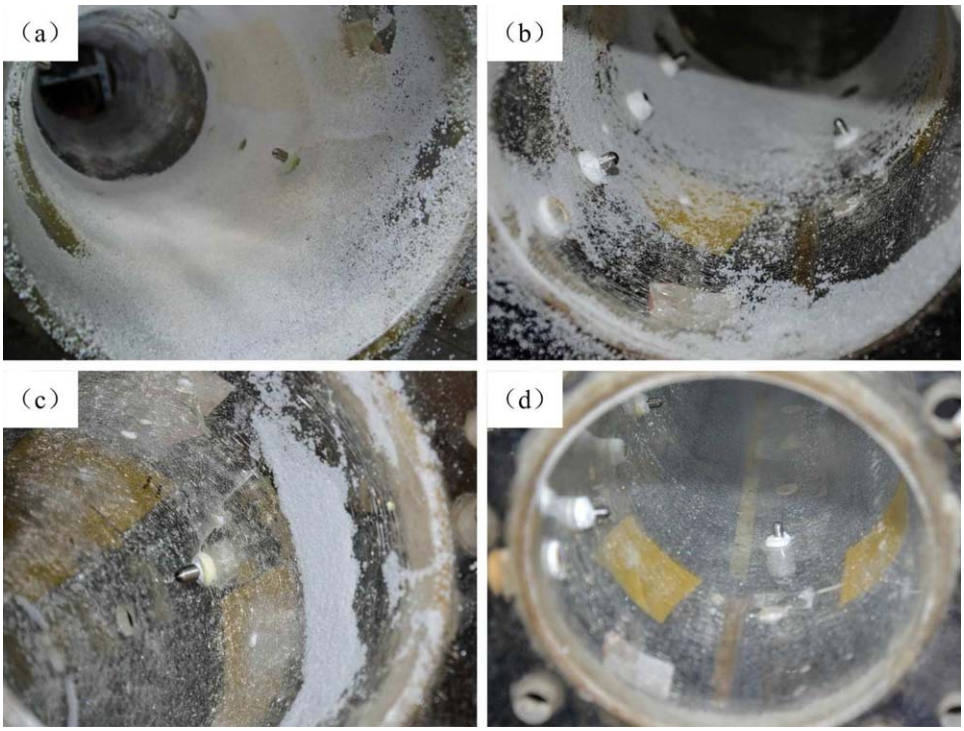

Figure 10. Wall sheeting in the fluidized bed with various LAA contents.

(a-0 ppm; b-12.5 ppm; c-25 ppm; d-50 ppm). [Color figure can be viewed in the online issue, which is available at wileyonlinelibrary.com.]

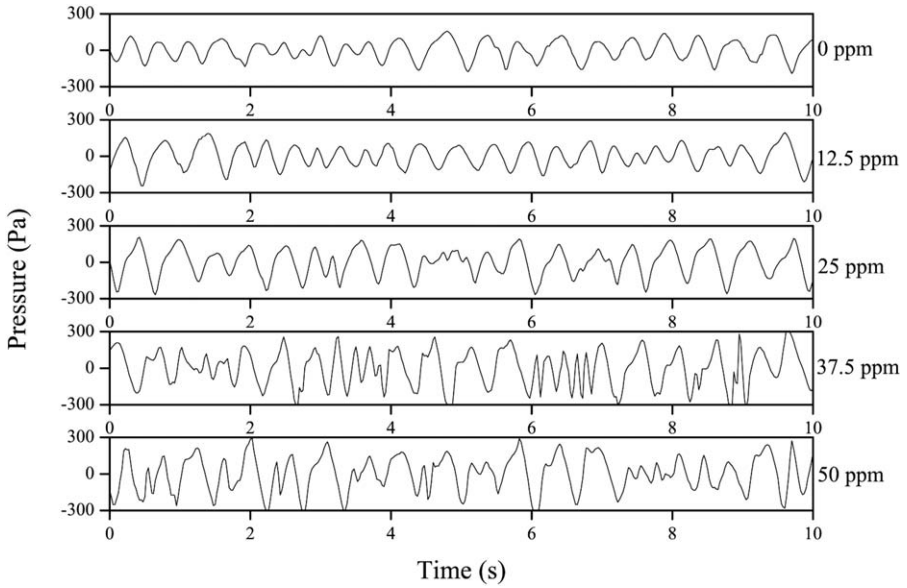

Figure 11. Pressure fluctuations at 160 mm under various contents of LAA. (0–55 ppm).

found which was consistent with the few changes of electrostatic charges in the fluidized bed. When the injection content of LAA increased, the periodicity of pressure signal decreased and the peak values were no more uniform. Meanwhile, a strong fluctuation of dynamic bed height and particles projection was experimentally observed. As can be seen from Figure 11, the pressure fluctuations with charged particles fluidized were quite distinct from those with neutralized particles. To the best of our knowledge, this phenomenon has not been reported before. Further analysis of pressure fluctuations were carried out below.

Figure 12 displays the probability density distributions (PDDs) of pressure fluctuations at 16 cm under various contents of LAA. As shown in Figure 12a, the PDDs under free fluidization differed from Gaussian distribution, offset to the right and were close to an approximate bimodal distribution. The PDDs narrowed when the fluidization time increased from 5–30 min. As analyzed, electrostatic charges increased with fluidization time until reaching equilibrium charge. After injection of LAA, the PDDs broadened, which indicated a larger fluctuation of pressures. With the increasing contents of LAA, the PDDs of pressure fluctuations broadened gradually and the approximate bimodal distribution turned to wide distribution finally. Fan et al.[37] indicated that the PDDs of pressure fluctuations were wider in the middle of the bed due to coexistence of small and large gas bubbles. When particles were monocharged, the electrostatic repulsion between charged particles resulted in an increased voidage of emulsion phase and gas bubbles were shrunk.[22] Thus, the PDDs of pressure fluctuations narrowed. From Section Electrostatic Charges Control Via LAA Injection, it is known that electrostatic charges decreased with the increasing injection content of LAA. Therefore, the constraints of charged particles on gas bubbles weakened and the PDDs widened with increasing content of LAA. When the injection content was larger than 37.5 ppm, charges of particles were almost completely eliminated and a further increase of injection content would not change the PDDs.

Figure 13 shows the variations of skewness of pressure fluctuations with increasing weight ratios of LAA. The negative value of skewness indicated a right offset of pressure fluctuations, as also shown in Figure 12. The skewness of pressure fluctuations for charged particles was smaller than that for fresh particles. After injection of LAA, the skewness increased with the decreased charge until the charged particles were completely neutralized. Abbasi et al.[38] found that the skewness of pressure fluctuations increased with the increasing superficial gas velocity, indicating a larger bubble size and stronger bubble motion resulted in a larger skewness. Therefore, it can be conjectured that charge reduction on particles leaded to a stronger bubble motion and a larger bubble size.

The standard deviation of pressure fluctuations was frequently used to qualitatively characterize the gas bubble size in the gas solid fluidized bed.[39,40] Figure 14a shows the variations of standard deviation of pressure fluctuations at 16 cm above the gas distributor before and after injection of 50 ppm LAA. At the beginning, the standard deviation decreased with fluidization time and reached its minimum after 10 min. After injection of 50 ppm for 20 min, the standard deviation rose quickly and reached its maximum at 26 min. In combination with the charge variations in Section Electrostatic Charges Control Via LAA Injection, it can be concluded that a large amount of charges on particles leaded to a decrease in gas bubble sizes and on the contrary, charge reduction resulted in bubble growth. Through DEM simulation, Hassani et al.[22] found that when particles were monocharged or nonequally bipolar charged, the electrostatic repulsion between charged particles could cause an increase of emulsion voidage and a decrease of gas bubble size. This is consistent with our experimental results. Moreover, the standard deviation increased with the increasing contents of LAA injected, as shown in Figure 14b. Therefore, a smaller amount of charges on particles caused a larger gas bubble in the fluidized bed.

It is difficult to obtain the diameters of gas bubbles in the three-dimensional fluidized bed experimentally. Van der Schaaf et al.[41,42] developed a decoupling method for analyzing pressure fluctuations, from which the bubble sizes can be estimated. On the other hand, Mori and Wen[43] developed a

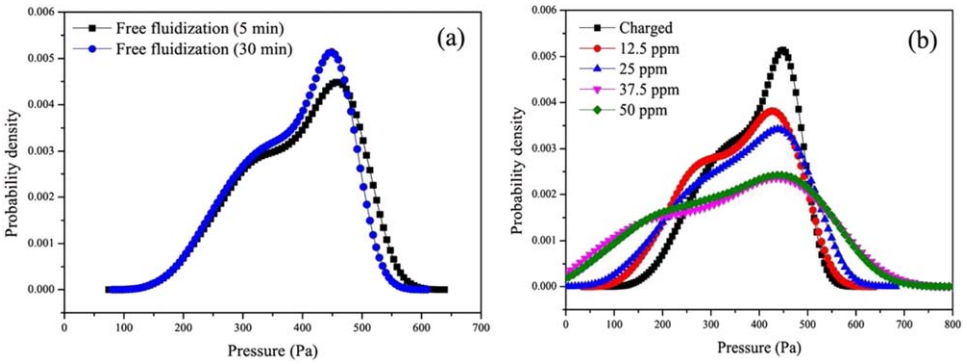

Figure 12. PDD of pressure fluctuations at 160 mm above the distributor. (a-under different fluidization times and b-under various contents of LAA).

[Color figure can be viewed in the online issue, which is available at wileyonlinelibrary.com.]

typical bubble size correlation for both Geldart B and Geldart D particles, as shown in following equations

$$\frac{d_{bm}-d_b}{d_{bm}-d_{b0}}=e^{-0.3z/dt} \tag{4}$$

$$d_{bm}=0.65\left[\frac{\pi}{4}d_t^2(u_0-u_{mf})\right]^{0.4} \tag{5}$$

where d_{b0} and d_{bm} represents the initial bubble size and the maximum bubble size respectively, and d_b is the bubble size at a certain height. According to Eq. 5, under a same superficial gas velocity u_0, a larger minimum fluidization velocity u_{mf} resulted in a smaller bubble size. This is because that an increasing minimum fluidization velocity increases the gas flow in emulsion phase and decreases the gas flow in bubble phase.

Figure 15 displays the variations of gas bubble sizes at 16 cm above the gas distributor before and after injection of LAA. The solid blocks stand for experimental values estimated from pressure fluctuations using van der Schaaf's decoupling method[42] and the solid line represents correlation prediction results based on a minimum fluidization velocity of 0.47 m/s, when charges of particles were eliminated by LAA. As shown in Figure 15, the bubble size decreased with fluidization time. When particles were fully charged, the bubble size decreased by 21% compared to that for fresh particles. After injection of 37.5 ppm LAA, the electrostatic charges decreased and the bubble size increased. During the 15 min after injection of LAA, the bubble diameter increased from 4.8 to 7.2 cm. The variation of bubble sizes was consistent with the results of skewness and standard deviations of pressure fluctuations. Therefore, electrostatic charges in the fluidized bed have a significant influence on bubble sizes and fewer charges facilitate bubble growth.

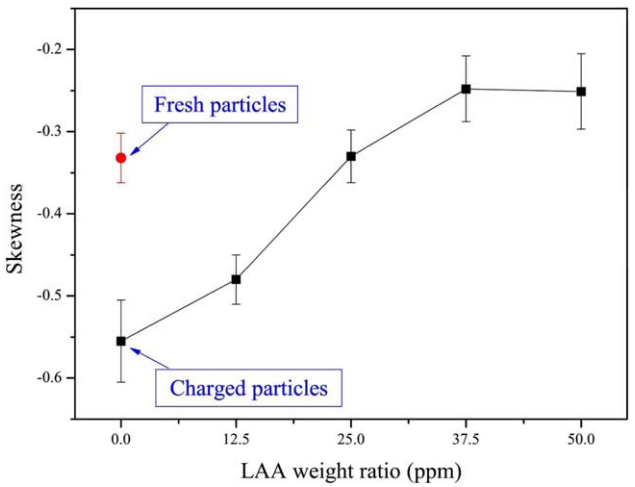

Figure 13. Skewness of pressure fluctuations at 16 cm under various LAA weight ratios.

[Color figure can be viewed in the online issue, which is available at wileyonlinelibrary.com.]

Besides, the correlation prediction of bubble size was obviously larger than the experimental values when particles were charged. This is due to the fact that the typical Mori–Wen's correlation did not consider the electrostatic effect on bubble sizes. Figure 16 further shows a comparison of bubble diameters between correlation predictions and experimental values obtained from pressure fluctuations. The solid line and dash line stand for correlation predictions with a minimum fluidization velocity of 0.47 and 0.54 m/s, respectively. As shown in Section Electrostatic Effect on Bubble Behaviors, the minimum fluidization velocity of PP particles raised from 0.47 to 0.54 m/s due to electrostatic charges. According to Mori–Wen's correlation, a larger u_{mf} leads to a smaller gas bubble size under an identical superficial gas velocity. When particles were freely charged, the bubble sizes were obviously smaller than correlation predictions. When adding 25 ppm LAA, the experimental value of bubble size was larger than the predicted value at $u_{mf}=0.54$ m/s. When the injection content reached 37.5 ppm, the experimental value was larger than the predicted value at $u_{mf}=0.47$ m/s. The discrepancy between predicted value and experimental value decreased after partial reduction of electrostatic charge. This result further verified the conclusion that neglecting consideration of electrostatic effect on the bubble sizes resulted in the discrepancy between correlation predicated value and experimental value.

To be concluded, the bubble size in the fluidized bed was reduced by electrostatics in two aspects: (1) Electrostatic repulsion force between charged particles leads to an increase of emulsion voidage and a decrease of bubble phase and (2) Electrostatic charges cause an increase of minimum fluidization velocity and lead to a decrease of bubble sizes.

Electrostatic effect on fluctuation of dynamic bed height

When particles were charged (free fluidization for 30 min), it was experimentally observed that the fluctuation of dynamic bed height was significantly reduced. However, the

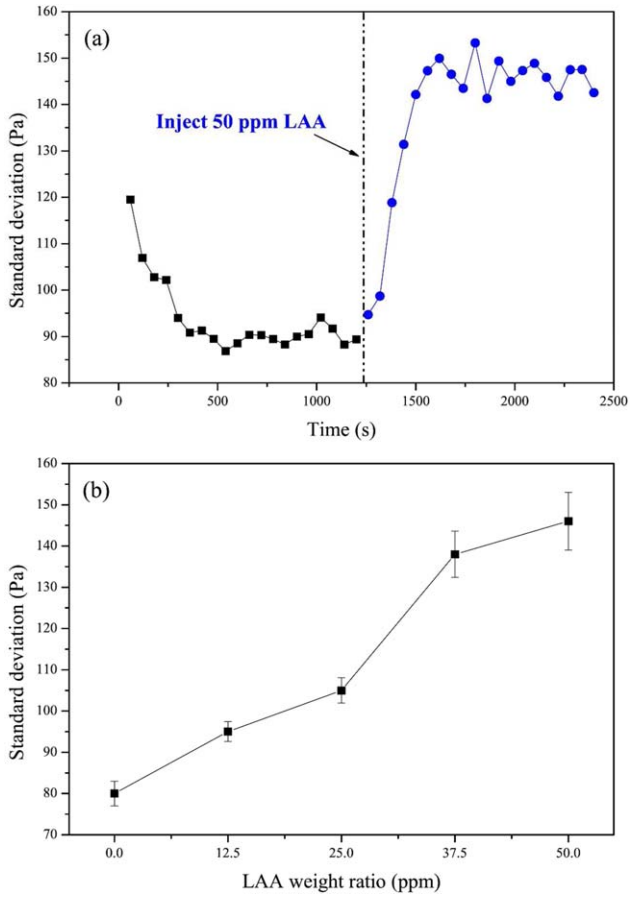

Figure 14. Standard deviation of pressure fluctuations at 160 mm.

(a) Variations of standard deviation with time before and after adding 50 ppm LAA and (b) Variations of mean standard deviation with LAA weight ratio. [Color figure can be viewed in the online issue, which is available at wileyonlinelibrary.com.]

dynamic bed height regained fluctuation after injection of 37.5 ppm LAA. During the experiments, fluctuation of dynamic bed height was simultaneously recorded by digital

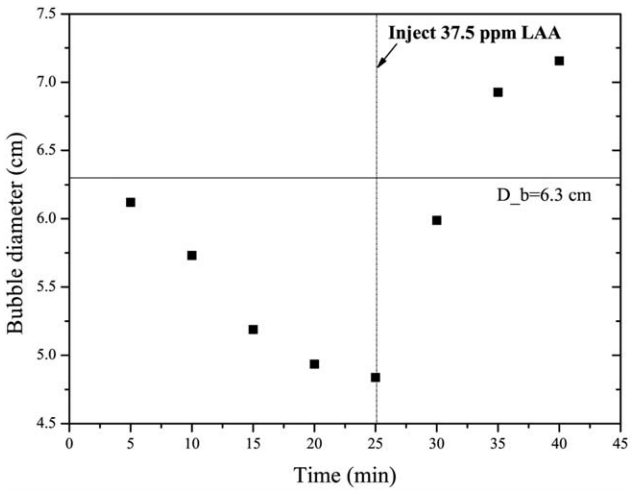

Figure 15. Variations of gas bubble sizes with time before and after injection of 37.5 ppm LAA.

[Color figure can be viewed in the online issue, which is available at wileyonlinelibrary.com.]

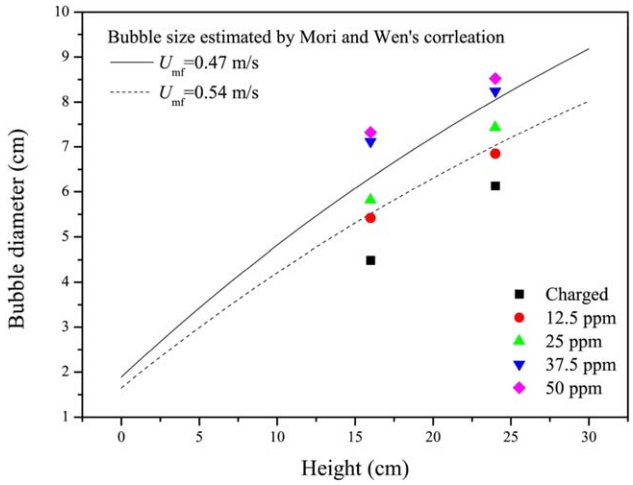

Figure 16. Comparison of bubble diameters with axial bed heights between correlation predictions and experimental values from pressure fluctuations under various weight ratios of LAA.

[Color figure can be viewed in the online issue, which is available at wileyonlinelibrary.com.]

camera as well as pressure fluctuations. Figure 17 shows a comparison of fluctuations of dynamic bed height obtained when particles were charged and neutralized. For charged particles, a smaller mean dynamic bed height can be found and the dynamic bed height was less fluctuating, compared to that for neutralized particles. When particles were charged, the bubbles in the bed were shrunk and the bubble size decreased, which resulted in a decrease of bubble rising velocity. Therefore, the dynamic bed height was less fluctuating for charged particles.

Van der Schaaf et al.[40] indicated the average cycle frequency (the reciprocal average cycle time [ACT]) was linearly proportional to the correlation entropy, which can be used to characterize the frequency of gas bubble eruption at bed surface. Figure 18 shows the variations of the ACT of pressure fluctuations with LAA weight ratios. The ACT is defined as twice the total sampling time divided by the number of crossings with the average value. When particles were charged, the relevant pressure fluctuations had a largest ACT, which indicated a most weak fluctuation of bed height. Furthermore, the ACT decreased with the increasing injection of LAA. The fluctuation of dynamic bed height was strongly relevant to the bubble size and bubble rise velocity. When charges of particles were neutralized, the bubble size increased and the bubble rise velocity was also increased. Therefore, the fluctuations of bed surface were strengthened when adding LAA.

Mechanism of electrostatic effect

Influences of electrostatic charges on bubble behaviors and bed surface fluctuations were investigated in Sections Electrostatic Effect on Bubble Behaviors and Electrostatic Effect on Fluctuation of Dynamic Bed Height, respectively. In conclusion, electrostatics had a severe effect on hydrodynamics in the fluidized bed. When particles were charged, the minimum fluidization velocity increased, bubble sizes decreased, and bed surface fluctuation weakened. The more charges the particles acquired, the more significant the

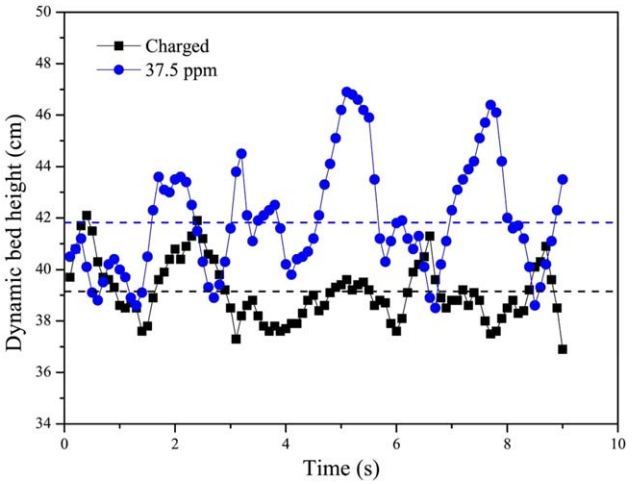

Figure 17. Fluctuations of dynamic bed heights.

[Color figure can be viewed in the online issue, which is available at wileyonlinelibrary.com.]

electrostatic effect was. Therefore, when considering the electrostatic effect in the fluidized bed, influence on hydrodynamics should be taken into more consideration than wall sheeting and agglomeration.

Electrostatic effect on bubble behaviors can be divided into two steps: (1) Influence of electrostatic force on the movement and distribution of charged particles and (2) Influence of particles movement and distribution on bubble behaviors. To explain how electrostatic charges affect the bubble behaviors in the fluidized bed, three simple cases are designed and displayed in Figure 19.

Case 1: Two monocharged particles in infinite space. According to Coulomb's law, the electrostatic force between charged particles is strongly influenced by charge amount and distance between two particles, as shown in Eq. 6

$$f_e = \frac{1}{4\pi\varepsilon_0}\frac{q_1 q_2}{r^2} \tag{6}$$

When two particles are monocharged, particles move away from each other to decrease the repulsion force. Therefore, the distance between two particles increases.

Case 2: N particles in limited space. The electrostatic force of particle i arising from other charged particles can be

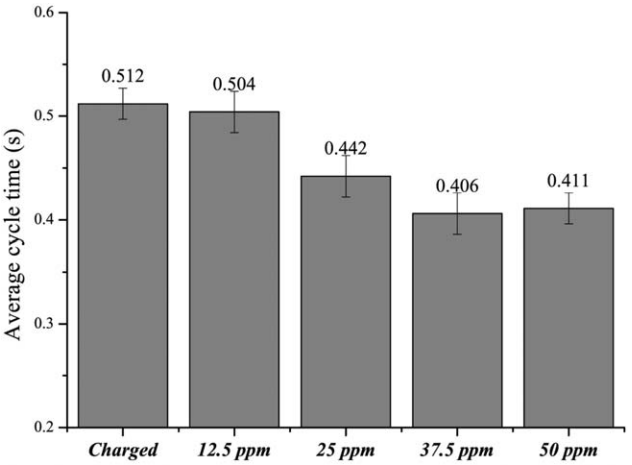

Figure 18. ACT of pressure fluctuations under various LAA weight ratios.

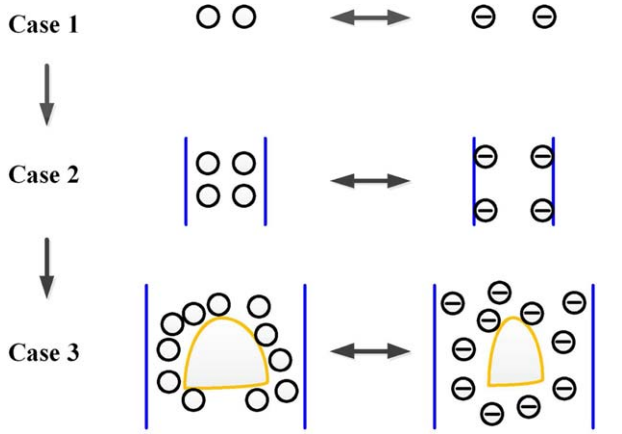

Figure 19. Schematic mechanism of electrostatic effect.

[Color figure can be viewed in the online issue, which is available at wileyonlinelibrary.com.]

calculated by assuming each particle to be a constant point charge, as shown in Eq. 7

$$f_{ep,i} = \sum_{\substack{j=1 \\ j\neq i}}^{N} \frac{q_i q_j}{4\pi\varepsilon_0 r_{ij}^2} \tag{7}$$

where r_{ij} is the mean distance between particle i and particle j. When all particles are monocharged, particles tend to move toward the interface and along the interface simultaneously. Thus the average repulsion force decreases and the mean distance among N particles increases.

Moreover, if the interface of limited space is also charged, supposing all charged particles are in an infinite cylinder (close to the fluidized bed), then the electrostatic force between particles and interface can be calculated as

$$f_{ew,i} = \frac{\lambda}{2\pi\varepsilon_0 r_{i,w}} q_i \tag{8}$$

where λ is the linear charge density of the interface and $r_{i,w}$ is the mean distance between particle i and the interface. If the interface has an opposite charge polarity with particles, the attraction force between particle and the wall, and repulsion force between particles and particles, make particles move toward interface more easily. Otherwise, if the interface and particles have identical polarity, the mean distance will be reduced to balance the repulsion force between particles and wall.

Case 3: N particles in a limited space with a gas bubble in the middle. If all the particles are monocharged, the repulsion forces between particles would increase the mean distance, thus the gas bubble is shrunk and larger repulsion forces will cause a larger decrease in bubble sizes. Moreover, if the interface and particles have opposite polarity, particles tend to adhere to the interface.

The gas-solid fluidized bed is somehow similar to the limited space in Case 3. When particles are mainly charged with one polarity, the repulsion force dominates. Therefore, particles are separated and bubbles are shrunk. Moreover, most particles in the bed have a charge polarity opposite to the wall.[16,34] The repulsion force between particle–particle and attraction force between particle-wall make particles easily adhere to the wall, which causes wall sheeting further. The stronger interaction between particles and the wall also causes a small increase in minimum fluidization velocity.

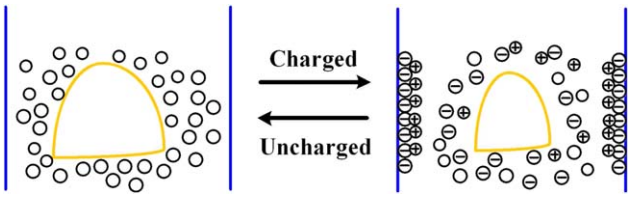

Figure 20. Electrostatic effects on gas bubble and wall sheeting.

[Color figure can be viewed in the online issue, which is available at wileyonlinelibrary.com.]

Conversely, if particles are mainly bipolar charged due to particle–particle collisions,[44,45] the attraction forces between bipolar charged particles would decrease the mean distance and increase the bubble sizes.[22] In other words, electrostatic effect of bipolar charge is contradictory to our experimental results. Therefore, electrostatic influence of mono charge was discussed in this work. This is because that more than 92% of fluidized particles have a diameter larger than 1 mm and triboelectric charging between PP and PMMA is more significant than particle–particle interactions due to a larger contact potential difference between different materials. Further experimental investigation of electrostatic effect of bipolar charge on bubble behaviors will be carried out in the future.

For our experimental system, particles were mainly negatively charged and the electrostatic effect was illustrated on the right of Figure 20. When injecting 37.5 ppm LAA, charges of particles were almost completely neutralized and the electrostatic effect disappeared.

Conclusions

Due to the difficulty in quantitatively controlling the degree of triboelectrification of insulated particles, there is a serious lack of experimental investigation of electrostatic effects on hydrodynamics in the fluidized bed. This work developed a new method to quantitatively adjust the charges of particles inside the fluidized bed by injecting a trace of LAAs and provided a first insight into the electrostatic effects on hydrodynamics experimentally. The main results are concluded as follows:

1. PP particles were mainly negatively charged in the freely bubbling fluidized bed. Injecting a trace of LAA caused obvious decrease of electrostatic charges and reduction or even disappearance of wall sheeting. The feasibility of controlling electrostatic charges via injecting LAA was first verified based on the variations of electrostatic voltage, charge-to-mass ratios and wall sheeting. The obtained data confirmed the probability and feasibility of adjusting the electrification degree of particles quantitatively by adding LAA, which laid the foundation of investigating electrostatic effects in the fluidized bed through experimental method.

2. Electrostatics had a severe effect on hydrodynamics in the fluidized bed. When increasing the degree of electrification of particles, which were mainly negatively charged, the minimum fluidization velocity increased, bubble sizes decreased and bed surface fluctuation weakened. The electrostatic effect became more prominent when particles were more charged.

3. Based on the results obtained, it is demonstrated that the influence of electrostatic charges on hydrodynamics arises from the variations of particle motion and distribution. When particles are mainly charged with one polarity, the repulsion force dominates. Then particles are separated and the void fraction in the emulsion phase increases, which indicates that bubbles are shrunk. The repulsion force among charged particles and particle-wall attraction force make particles easily adhere to the wall.

When considering the electrostatic effect in the fluidized bed, besides wall sheeting and agglomeration, the influence of electrostatics on hydrodynamics should also be taken into more consideration. Electrification of particles can cause remarkable decreases of bubble size and rising velocity. Moreover, the fluctuation of the bed is weakened and the fluidization quality declines. Therefore, it is of vital importance to reduce or even avoid electrostatic charge accumulation in the industrial fluidized bed reactors.

Acknowledgment

The authors are grateful for the financial support of this wok from the National Natural Science Foundation of China (Grant No. 21236007), National Basic Research Program of China (Grant No. 2012CB720500), Specialized Research Fund for the Doctoral Program of Higher Education (Grant No. 20130101110063) and Zhejiang Provincial Natural Science Foundation of China (Grant No. LQ13B060002).

Literature Cited

1. Hendrickson G. Electrostatics and gas phase fluidized bed polymerization reactor wall sheeting. *Chem Eng Sci*. 2006;61(4):1041–1064.
2. Wang F, Wang J, Yang Y. Distribution of electrostatic potential in a gas-solid fluidized bed and measurement of bed level. *Ind Eng Chem Res*. 2008;47:9517–9526.
3. Boland D, Geldart D. Electrostatic charging in gas fluidised beds. *Powder Technol*. 1972;5(5):289–297.
4. Park A-H, Bi H, Grace JR. Reduction of electrostatic charges in gas-solid fluidized beds. *Chem Eng Sci*. 2002;57(1):153–162.
5. Zhao H, Castle GSP, Inculet II. The measurement of bipolar charge in polydisperse powders using a vertical array of Faraday pail sensors. *J Electrostatics*. 2002;55(3–4):261–278.
6. Mehrani P, Bi HT, Grace JR. Electrostatic charge generation in gas-solid fluidized beds. *J Electrostatics*. 2005;63(2):165–173.
7. Chen A, Bi H, Grace JR. Effects of probe numbers and arrangement on the measurement of charge distributions around a rising bubble in a two-dimensional fluidized bed. *Chem Eng Sci*. 2006;61:6499–6510.
8. Chen A, Bi HT, Grace JR, Van Willigen FK, Van Ommen JR. Measurement of charge distribution around a rising bubble in a 2-D fluidized bed. *AIChE J*. 2006;52:174–184.
9. Sowinski A, Salama F, Mehrani P. New technique for electrostatic charge measurement in gas-solid fluidized beds. *J Electrostatics*. 2009;67:568–573.
10. Sowinski A, Miller L, Mehrani P. Investigation of electrostatic charge distribution in gas-solid fluidized beds. *Chem Eng Sci*. 2010; 65:2771–2781.
11. Moughrabiah WO, Grace JR, Bi XT. Effects of pressure, temperature, and gas velocity on electrostatics in gas-solid fluidized beds. *Ind Eng Chem Res*. 2009;48(1):320–325.
12. Yu X, Li W, Xu Y, Wang J, Yang Y, Xu N, Wang H. Effect of polymer granules on the electrostatic behavior in gas-solid fluidized beds. *Ind Eng Chem Res*. 2010;49:132–139.
13. Moughrabiah WO, Grace JR, Bi XT. Electrostatics in gas–solid fluidized beds for different particle properties. *Chem Eng Sci*. 2012;75: 198–208.
14. Sowinski A, Mayne A, Mehrani P. Effect of fluidizing particle size on electrostatic charge generation and reactor wall fouling in gas–solid fluidized beds. *Chem Eng Sci*. 2012;71:552–563.
15. Zhou Y, Ren C, Wang J, Yang Y, Dong K. Effect of hydrodynamic behavior on electrostatic potential distribution in gas–solid fluidized bed. *Powder Technol*. 2013;235:9–17.
16. Matsusaka S, Maruyama H, Matsuyama T, Ghadiri M. Triboelectric charging of powders: a review. *Chem Eng Sci*. 2010;65(22):5781–5807.
17. Wang J, Xu Y, Li W, Yang Y, Wang F. Electrostatic potentials in gas-solid fluidized beds influenced by the injection of charge inducing agents. *J Electrostatics*. 2009;67:815–826.

18. Rokkam RG, Fox RO, Muhle ME. Computational fluid dynamics and electrostatic modeling of polymerization fluidized-bed reactors. *Powder Technol*. 2010;203:109–124.
19. Briens CL, Bergougnou MA, Inculet II, Baron T, Hazlett JD. Size distribution of particles entrained from fluidized beds: electrostatic effects. *Powder Technol*. 1992;70(1):57–62.
20. Li J, Kato K. Effect of electrostatic and capillary forces on the elutriation of fine particles from a fluidized bed. *Adv Powder Technol*. 2001;12(2):187–205.
21. Jalalinejad F, Bi XT, Grace JR. Effect of electrostatic charges on single bubble in gas–solid fluidized beds. *Int J Multiphase Flow*. 2012;44:15–28.
22. Hassani MA, Zarghami R, Norouzi HR, Mostoufi N. Numerical investigation of effect of electrostatic forces on the hydrodynamics of gas–solid fluidized beds. *Powder Technol*. 2013;246:16–25.
23. Lim EWC. Mixing behaviors of granular materials in gas fluidized beds with electrostatic effects. *Ind Eng Chem Res*. 2013;52(45):15863–15873.
24. Castle GSP. Contact charging between insulators. *J Electrostatics*. 1997;40–41:13–20.
25. Huiliang Z, Castle GSP, Inculet II, Bailey AG. Bipolar charging of poly-disperse polymer powders in fluidized beds. *IEEE Trans Ind Appl*. 2003;39(3):612–618.
26. Beetstra R, Nijenhuis J, Ellis N, van Ommen JR. The influence of the particle size distribution on fluidized bed hydrodynamics using high-throughput experimentation. *AIChE J*. 2009;55(8):2013–2023.
27. Kok JF, Lacks DJ. Electrification of granular systems of identical insulators. *Phys Rev E*. 2009;79(5):051304.
28. McLaughlin LJ, Rhodes MJ. Prediction of fluidized bed behaviour in the presence of liquid bridges. *Powder Technol*. 2001;114(1–3):213–223.
29. Itakura T, Masuda H, Ohtsuka C, Matsusaka S. The contact potential difference of powder and the tribo-charge. *J Electrostatics*. 1996;38(3):213–226.
30. Nomura T, Satoh T, Masuda H. The environment humidity effect on the tribo-charge of powder. *Powder Technol*. 2003;135–136:43–49.
31. Ciborowski J, Wlodarski A. On electrostatic effects in fluidized beds. *Chem Eng Sci*. 1962;17(1):23–32.
32. Cross J. Electrostatics: principles, problems and applications. Bristol: Adam Hilger; 1987.
33. Giffin A, Mehrani P. Effect of gas relative humidity on reactor wall fouling generated due to bed electrification in gas-solid fluidized beds. *Powder Technol*. 2013;235(0):368–375.
34. Salama F, Sowinski A, Atieh K, Mehrani P. Investigation of electrostatic charge distribution within the reactor wall fouling and bulk regions of a gas–solid fluidized bed. *J Electrostatics*. 2013;71(1):21–27.
35. Wang J, Cao Y, Jiang X, Yang Y. Agglomeration detection by acoustic emission (AE) sensors in fluidized beds. *Ind Eng Chem Res*. 2009;48(7):3466–3473.
36. Jingdai W, Congjing R, Yongrong Y. Characterization of flow regime transition and particle motion using acoustic emission measurement in a gas-solid fluidized bed. *AIChE J*. 2010;56(5):1173–1183.
37. Fan LT, Ho T-C, Hiraoka S, Walawender WP. Pressure fluctuations in a fluidized bed. *AIChE J*. 1981;27(3):388–396.
38. Abbasi M, Sotudeh-Gharebagh R, Mostoufi N, Zarghami R, Mahjoob MJ. Nonintrusive characterization of fluidized bed hydrodynamics using vibration signature analysis. *AIChE J*. 2010;56(3):597–603.
39. van der Schaaf J, Schouten JC, van den Bleek CM. Origin, propagation and attenuation of pressure waves in gas–solid fluidized beds. *Powder Technol*. 1998;95(3):220–233.
40. van der Schaaf J, van Ommen JR, Takens F, Schouten JC, van den Bleek CM. Similarity between chaos analysis and frequency analysis of pressure fluctuations in fluidized beds. *Chem Eng Sci*. 2004;59:1829–1840.
41. van der Schaaf J, Schouten JC, Johnsson F, van den Bleek CM. Non-intrusive determination of bubble and slug length scales in fluidized beds by decomposition of the power spectral density of pressure time series. *Int J Multiphase Flow*. 2002;28(5):865–880.
42. Chilekar VP, Warnier MJF, van der Schaaf J, Kuster BFM, Schouten JC, van Ommen JR. Bubble size estimation in slurry bubble columns from pressure fluctuations. *AIChE J*. 2005;51(7):1924–1937.
43. Mori S, Wen C. Estimation of bubble diameter in gaseous fluidized beds. *AIChE J*. 1975;21(1):109–115.
44. Lacks DJ, Duff N, Kumar SK. Nonequilibrium accumulation of surface species and triboelectric charging in single component particulate systems. *Phys Rev Lett*. 2008;100(18):188305.
45. Forward KM, Lacks DJ, Sankaran RM. Particle-size dependent bipolar charging of Martian regolith simulant. *Geophys Res Lett*. 2009;36(13):L13201.

Manuscript received July 20, 2014, and revision received Dec. 21, 2014.